

**Fast response cavity enhanced ozone monitor**

A. L. Gomez and  
E. P. Rosen

This discussion paper is/has been under review for the journal Atmospheric Measurement Techniques (AMT). Please refer to the corresponding final paper in AMT if available.

# Fast response cavity enhanced ozone monitor

**A. L. Gomez and E. P. Rosen**

Southwest Sciences, Inc., 1570 Pacheco St. Ste. E-11, Santa Fe, NM, USA

Received: 6 September 2012 – Accepted: 17 September 2012  
– Published: 26 September 2012

Correspondence to: A. L. Gomez (algomez@swsciences.com)

Published by Copernicus Publications on behalf of the European Geosciences Union.

Title Page

Abstract

Introduction

Conclusions

References

Tables

Figures

⏪

⏩

◀

▶

Back

Close

Full Screen / Esc

Printer-friendly Version

Interactive Discussion

## Abstract

Ozone is an important atmospheric gas due to its role in air quality and radiative forcing. A new method for sensitive, rapid monitoring of ambient ozone has been developed using a compact platform and relatively inexpensive components. Based on Incoherent Broadband Cavity Enhanced Absorption Spectroscopy (IBB-CEAS), the device utilizes an optical cavity of just 14.5 cm and moderately high reflectivity mirrors ( $R = 99.3\%$ ). Performance of the instrument has been validated against direct absorption measurements in a single-pass measurement cell. Currently, the IBB-CEAS ozone instrument can achieve 1 ppb sensitivities at 0.1 s integration time with a dynamic range over four orders of magnitude, accessing relevant ozone concentrations in both the stratosphere and troposphere. This new device offers improved sensitivity and time response for mapping ozone aboard airborne platforms.

## 1 Introduction

Ozone, a tri-atomic oxygen molecule, is a highly reactive oxidant ubiquitous in the stratosphere and troposphere. Ozone concentrations and their impact are highly variable, depending on the strata of the atmosphere. Likewise, generation of ozone occurs by very different mechanisms depending on location. The need to measure distribution and concentration of ozone and to validate satellite based data is critical due to ozone's strong impact on health and climate forcing.

Ozone is naturally occurring in the stratosphere (0 to < 10 ppm) where it is generated by UV photolysis of  $O_2$  with Lyman-alpha radiation at 210 nm. By and large, stratospheric ozone is very beneficial due to its strong UV absorption for wavelengths shorter than about 290 nm. This actinic cutoff blocks most of the harmful solar UV radiation (Cullen and Neale, 1994). Ozone's impact on UV transmission is so important that elucidation of the mechanism leading to its destruction led to a Nobel Prize and resulted in global environmental controls on CFCs with the Montreal Protocol (Molina

AMTD

5, 7223–7241, 2012

### Fast response cavity enhanced ozone monitor

A. L. Gomez and  
E. P. Rosen

Title Page

Abstract

Introduction

Conclusions

References

Tables

Figures

⏪

⏩

◀

▶

Back

Close

Full Screen / Esc

Printer-friendly Version

Interactive Discussion



and Rowland, 1974). Stratospheric ozone is mainly lost via  $O_x$ ,  $NO_x$ ,  $HO_x$  and halogen radical chemistry (Wennberg et al., 1994). In the middle and upper stratosphere (above 30 km) the photochemical lifetime is short, on the order of days to a week, and the ozone concentration is determined by chemistry alone. In the lower stratosphere, the ozone lifetime becomes long and transport is critical for determining the local concentrations of ozone.

In the troposphere, ozone exists at low concentration ranging from  $\sim 10$  ppb in remote regions, to  $\sim 500$  ppb in extremely polluted urban environments. Its presence is driven by the processing of anthropogenic  $NO_x$  emissions (Sillman, 1999; Finlayson-Pitts and Pitts, 1997). Even at low concentrations, ozone is harmful and is monitored by the EPA as a criteria pollutant. It causes damage to various materials common in the urban environment, such as rubber (Braden and Gent, 1960), and it can damage the eyes and lungs of children (Gauderman et al., 2002) and animals. It has also been shown to be harmful to agriculture (Fuhrer and Booker, 2003). In addition to its influence on public health, tropospheric ozone also impacts climate. OH radicals formed by tropospheric ozone photolysis are key players in both the oxidation of volatile organic compounds (VOCs) and the aging/formation of organic and secondary organic aerosols.

Although slow compared to OH radical reactions, ozone's much larger concentration makes it a key player in VOC aging and secondary organic aerosol (SOA) formation. Ozonation of double bonds goes by way of the Criegee mechanism. The end result of this process is increased oxidation state and increased hydrophilicity of organics. When transported into the stratosphere, these SOAs serve as cloud condensation nuclei, which ultimately affect climate forcing by changing the earth's albedo.

Global ozone distributions are obtained from integrated satellite measurements from the NASA Ozone Monitoring instrument (which replaced NASA's Total Ozone Mapping Spectrometer). These measurements are important for tracking stratospheric ozone depletion and for understanding radiative forcing as ozone is one of the most important greenhouse gases after carbon dioxide. However, temporal resolution is severely

## Fast response cavity enhanced ozone monitor

A. L. Gomez and  
E. P. Rosen

[Title Page](#)[Abstract](#)[Introduction](#)[Conclusions](#)[References](#)[Tables](#)[Figures](#)[Back](#)[Close](#)[Full Screen / Esc](#)[Printer-friendly Version](#)[Interactive Discussion](#)

**Fast response cavity enhanced ozone monitor**A. L. Gomez and  
E. P. Rosen

Title Page

Abstract

Introduction

Conclusions

References

Tables

Figures

⏪

⏩

◀

▶

Back

Close

Full Screen / Esc

Printer-friendly Version

Interactive Discussion



limited to daily time scales. To improve radiative models, temporal resolution of data needs to be substantially improved, as stratospheric ozone concentrations can change significantly on the hour time scale. Additionally, tropospheric ozone is very difficult to extract from satellite data due to its small contribution to the total integrated signal, and it varies on an even faster time scale than stratospheric ozone. Thus, instrumentation is needed that can validate and support satellite measurements through sensitive in situ ozone measurements on airborne platforms at increased spatial and temporal resolution.

Traditional optical ozone instruments are limited in their ability to both rapidly and sensitively measure ozone. These instruments are based on direct absorption of UV light by ozone, which has an absorption cross-section of  $1.15 \times 10^{-17} \text{ cm}^2 \text{ molec}^{-1}$  at 254 nm (Molina and Molina, 1986). The intensity of the transmitted light through an optically transparent sample cell is compared to the transmitted intensity when the ozone has been neutralized by means of an ozone neutralizer such as a carbon filter. Highly sensitive measurements require a long optical path, leading to large instrument sample volume. The long temporal response required to exchange the sample volume prevents detection of rapidly varying ozone concentrations.

Alternative approaches commonly used for ozone measurement, including chemiluminescence and iodometric electrochemistry, have shortcomings for deployment on airborne platforms. Chemiluminescence can be generated through reaction of ozone with NO (Ridley et al., 1992) or an organic dye (Zahn et al., 2012) and offers a fast response (1–20 Hz), but requires regular calibration at longer timescales by an absolute sensor. Electrochemical Concentration Cells (Komhyr, 1969) are compact devices capable of use as balloonsondes, but require a longer measurement time (1 Hz) and decay of cell current can lead to systematic biasing of measurements at low concentrations (Vömel and Diaz, 2010). Neither of these methods offers an absolute ozone measurement, and each requires consumables for operation and calibration that limit suitability for long duration operation.

**Fast response cavity enhanced ozone monitor**A. L. Gomez and  
E. P. Rosen

Title Page

Abstract

Introduction

Conclusions

References

Tables

Figures

⏪

⏩

◀

▶

Back

Close

Full Screen / Esc

Printer-friendly Version

Interactive Discussion



Resonant optical cavities can overcome limitations of direct absorbance measurements, reducing the physical size of an instrument while maintaining the long optical paths requisite for high sensitivity measurements. Recently, Washenfelder et al. developed a cavity ring-down instrument for ozone detection based on a high finesse optical cavity (Washenfelder et al., 2011). While the instrument offers a very low limit of detection (26 ppt ozone), this approach relies on converting ozone to  $\text{NO}_2$  through a reaction cell, increasing the instrument size and requiring calibration gases. We offer an alternative resonant cavity to measure ozone at both high sensitivity and high speed, using relatively inexpensive UV-LEDs and requiring no consumables.

Incoherent broadband cavity enhancement absorption spectroscopy (IBB-CEAS) takes advantage of spectrally broad light, overlapping hundreds to thousands of resonant cavity modes, to generate a continuous transmission signal having an enhanced absorption response characteristic of a much longer physical pathlength. IBB-CEAS has been used to make sensitive measurements of trace atmospheric gases (Venables et al., 2005; Gherman et al., 2008; Wu et al., 2008), but we believe this to be the first application of the technique to measurement of ozone. Novel CEAS measurements of ozone have been obtained recently using an atomic line source, and achieved a sensitivity of  $\sim 8$  ppb at 10 s with a 25 cm cavity (Darby et al., 2012). Here, we present results from a compact 14.5 cm optical measurement cell, yielding IBB-CEAS ozone measurements of  $\sim 1$  ppb sensitivity at 0.1 s.

## 2 Experimental setup

### 2.1 Principle of operation

The transmission intensity ( $I$ ) of light through an optical cavity, consisting of mirrors with reflectivity  $R$ , can be described (Fiedler et al., 2003) as the superposition of the sum of discrete transmitted light per pass. Transmission losses arise from the mirrors

$(1 - R)$  and the load loss of the cavity  $L$ , where  $L$  is the single pass loss. The observed transmission intensity is related to the intensity of light into the cavity,  $I_{in}$ , according to:

$$I = I_{in} \frac{(1 - R)^2 (1 - L)}{1 - R^2 (1 - L)^2} \quad (1)$$

For an unloaded cavity ( $L = 0$ ), this reduces to:

$$I_o = I_{in} \frac{(1 - R)}{(1 + R)} \quad (2)$$

Hence, the cavity transmission ( $T$ ) is:

$$T = \frac{I}{I_o} = \frac{1 - R^2}{1 - R^2 (1 - L)^2} \quad (3)$$

The cavity enhancement gained from using a resonant cell versus a typical single pass cell can be expressed as the ratio of the transmission loss to the single pass loss:

$$E = \frac{I/I_o}{(1 - L)} \quad (4)$$

Conveniently, the enhancement gains are greatest when the loss is the smallest. This low loss enhancement is what allows exceptional sensitivity in a compact absorption cavity.

## 2.2 Technical design

The IBB-CEAS system consists of: (1) UV source/detection; (2) measurement cells (resonant and single pass reference); (3) flow handling; and, (4) ozone generation/neutralization. The instrument was built upon the ThorLabs 30 mm cagemount system to facilitate breadboard design and provide ruggedness. The measurement portion of the system can be seen in Fig. 1.

### Fast response cavity enhanced ozone monitor

A. L. Gomez and  
E. P. Rosen

Title Page

Abstract

Introduction

Conclusions

References

Tables

Figures

⏪

⏩

◀

▶

Back

Close

Full Screen / Esc

Printer-friendly Version

Interactive Discussion





to evaluate instrument performance. Concentrations of ozone within the reaction cell could be varied by altering the discharge current to the lamp, and mixing ratios within the sample cells could be controlled by modulating the sampling time from the ozone reaction cell. When applicable, ozone was neutralized with an inline canister of high surface area granular carbon to evaluate  $I_o$ .

### 3 Results

The performance capability for measuring ozone with the IBB-CEAS technique was evaluated through direct comparison with a matching single-pass absorption measurement. The ozone reservoir was periodically sampled into the coupled IBB-CEAS and single-pass cells at various mixing ratios with ambient air to obtain a wide range of measured concentrations. Figure 2 shows the results from sampling bursts of ozone-laden air into the sample cells, illustrating the improvement in the signal-to-noise of the IBB-CEAS measurement over the single pass measurement. For the lowest concentration of measurements (0.1 s integration), the single pass measurements barely discern an ozone signal, while the IBB-CEAS measurement clearly show a transience in ozone concentration.

Comparison of the measured transmission losses between the cavity-enhanced cell and single-pass cell allows the enhancement gain from the IBB-CEAS measurement cell to be determined according to Eq. (4). These results, corrected for  $I_o$  drift, are shown in Fig. 3. An enhancement factor of 50-fold is clearly shown for the IBB-CEAS measurement with respect to the single pass measurement. Scatter at low loss is due to noise in the single pass measurements used in the calculation. The observed transmission loss in the single-pass and IBB-CEAS cell can be directly converted to an ozone concentration using the Beer-Lambert Law and measured enhancement factor. Here, the IBB-CEAS system demonstrates measurements from 300 ppb to 13 ppb with a standard deviation noise floor of  $< 1$  ppb ozone. These data, taken at 0.1 s integration time, also demonstrated the minimal averaging time required to achieve high sensitivity.

## Fast response cavity enhanced ozone monitor

A. L. Gomez and  
E. P. Rosen

Title Page

Abstract

Introduction

Conclusions

References

Tables

Figures

◀

▶

◀

▶

Back

Close

Full Screen / Esc

Printer-friendly Version

Interactive Discussion



**Fast response cavity enhanced ozone monitor**A. L. Gomez and  
E. P. Rosen

Title Page

Abstract

Introduction

Conclusions

References

Tables

Figures

◀

▶

◀

▶

Back

Close

Full Screen / Esc

Printer-friendly Version

Interactive Discussion



Lower ozone mixing ratios were explored by operating the ozone lamp at low current. Under this regime, the lamp transitions from quasi-continuous (very rapid pulses) to pulsed emission. When the current on the lamp's power supply output is adjusted to the lowest setting, the lamp undergoes periodic capacitive discharge, generating discrete bursts of light and ozone approximately every 4 s. Figure 4 demonstrates the detection of transient, low concentration ozone levels generated from the lamp flashes, which are rapidly diluted in the sample cells back to baseline as air is drawn through the system. These data, acquired at 100 Hz, show that IBB-CEAS is vastly superior to the single pass measurement, fully resolving the < 10 ppb ozone bursts with a limit of detection of ~ 1 ppb.

System stability, shown in Fig. 5, was determined from Allan deviation analysis. Data were acquired for 6000 s for both the amplifier (DC, LED off) and the stabilized cavity throughput ( $I_o$ , LED on) at 0.1 s integration time. The standard deviation was calculated for data binned from 0.1 s to 600 s of data averaging. Over the course of acquisition, the DC component from the amplifier was stable and showed no substantial long term drift. The  $I_o$  component of the system, which includes the DC component plus LED output stability and cavity coupling stability, had drift of  $\pm 0.2\%$  over 100 min. The system stability is well below an effective 1 ppb ozone concentration at 10 Hz, and only exceeds this threshold after approximately 400 s of integration.

## 4 Discussion

According to Eq. (3), the theoretical enhancement for a cavity consisting of mirrors with  $R = 99.3\%$  should approach a factor of 142 as cavity losses decrease. The data presented in Fig. 3 indicate that for small losses, the IBB-CEAS system has a measured enhancement of approximately 50 with respect to a single pass cell. This difference in enhancement may arise from one or a combination of the following sources: (1) cavity coupling; (2) Rayleigh scattering; and/or (3) out of band light (OBL). Each of these sources was evaluated systematically. Cavity coupling was investigated by changing

## Fast response cavity enhanced ozone monitor

A. L. Gomez and  
E. P. Rosen

Title Page

Abstract

Introduction

Conclusions

References

Tables

Figures

⏪

⏩

◀

▶

Back

Close

Full Screen / Esc

Printer-friendly Version

Interactive Discussion

the input conditions of the LED by varying the focal plane of the mode matching optics and by aperturing incident emission, neither of which provided a significant improvement on enhancement. Rayleigh scattering was calculated to be an insignificant loss term compared to the cavity loss at 255 nm ( $4 \times 10^{-5}$ ) and was verified with low pressure experiments. Out of band light (OBL), however, appears to explain the enhancement discrepancy. OBL is simply light generated from the LED measured by the photodetector falling outside the mirror reflectivity band, such that it has a considerably shorter effective path length through the cell than in band light. Since it is non-resonant (or lower resonant for light that sits on the shoulder of the reflectivity curve), OBL suppresses enhancement when it is averaged with the transmitted signal. We tested the effect of reducing OBL by comparing two SiC detectors, where one had a UV-C (220–275 nm) filter integrated in the package housing. Although the UV-C filter is not optimized to remove all OBL from the LED, this simple modification improved the enhancement from  $\sim 30\times$  to  $50\times$ . Future generations of the IBB-CEAS system will employ tailored filtering to further reject OBL, thereby improving system performance.

Measurement precision is often improved upon with signal averaging. For an ideal system limited by white noise, averaging can improve the signal-to-noise ratio by the square root of the number of averages. However, averaging gains are often limited by systematic sources such as thermal drift, that do not benefit from additional averaging. For IBB-CEAS, the precision is dependent on the stability of the DC component of the signal. In this system, it is the combination of stability from cavity coupling, LED output ( $I_{in}$ ), the amplifier, and detector responsivity. Contributions from any of these components to the DC signal cannot be averaged out and dictate the time scale for re-zeroing the measurement system for the condition of zero-ozone ( $I_o$ ). Figure 5 shows the total system stability ( $I_o$ ) and the effects of signal averaging. Allan deviation analysis on long period steady state measurements yield valuable information on practical system limits. Non-stochastic noise is the primary limitation in this system keeping the limit of detection to a few hundred ppt. The system drift also dictates a period of a few hundred

seconds for re-determining  $I_0$  with a zero-ozone measurement in order to maintain  $< 1$  ppb ozone detection.

We can estimate the full dynamic range of the IBB-CEAS measurement system, by approximating Eq. (3) to account for the OBL reduction of enhancement ( $50 \times$  enhancement  $\rightarrow R = 98\%$ ). If we define the dynamic range as the noise floor up to an absorbance of 1, for 0.1 s measurements, IBB-CEAS has a measurement capability from 1 ppb to  $\sim 15$  ppm. For a measurement system that paralleled IBB-CEAS with single pass measurements, the upper end would extend measurements to about 600 ppm. This parallel measurement would have the added benefit of self calibrating the enhancement factor for when IBB-CEAS and single pass both have appreciable transmission losses.

As a comparison, we can look at the performance of a well received commercial optical ozone monitor, the 2B Technologies Model 205 dual beam ozone monitor. This instrument is approved by the EPA as a Federal Equivalent Method for monitoring ozone. This instrument is also used by NOAA for their ESRL/GMD Tropospheric Aircraft Ozone Measurement Program, and by NASA/NOAA for measurements of ozone with the Global Hawk unmanned aircraft system. The Model 205 has a sensitivity of 3 ppb, a dynamic range of 1.5 ppb to 250 ppm, and response time of 10 s. The present IBB-CEAS system has a sensitivity of  $< 1$  ppb, a dynamic range of 1 ppb to 660 ppm (with tandem single pass measurement/calibration cell), and a measurement time of 0.1 s. This very fast response time could be particularly useful for airborne measurements where a significantly improved resolution for ozone mapping could be obtained.

## 5 Conclusions

The work presented here demonstrates a compact, self-calibrating optical instrument for absolute measurements of ozone at 1 ppb sensitivities at 0.1 s or faster with no consumables. These results are a substantial improvement over related single pass instrumentation (also operating at 255 nm) which typically takes a few seconds to a minute

### Fast response cavity enhanced ozone monitor

A. L. Gomez and  
E. P. Rosen

Title Page

Abstract

Introduction

Conclusions

References

Tables

Figures

⏪

⏩

◀

▶

Back

Close

Full Screen / Esc

Printer-friendly Version

Interactive Discussion



to attain a detection limit of a few ppb. The instrument is capable of sensitive measurements at ozone concentrations relevant to both the troposphere and the stratosphere. It is anticipated that simple improvements limiting the transmission of out of band light will provide further gains in sensitivity.

The high sensitivity and rapid measurement capabilities of the IBB-CEAS ozone monitor have clear applications for airborne platforms. With the ability to measure unique air samples at 10 Hz with 1 ppb sensitivities, the IBB-CEAS ozone measurement system will allow for one to two orders of magnitude improvement in spatial measurement resolution for airborne platforms currently using traditional optical instrumentation.

*Acknowledgements.* This manuscript has been authored by employees of Southwest Sciences, Inc. under Contract/Grant No NNX12CD23P with the National Aeronautics and Space Administration. The United States Government has a nonexclusive, irrevocable, worldwide license to prepare derivative works, publish or reproduce this manuscript, and allow others to do so, for United States Government purposes. Any publisher accepting this manuscript for publication acknowledges that the United States Government retains such a license in any published form of this manuscript. All other rights are retained by the copyright owner.

## References

- Braden, M. and Gent, A. N.: The attack of ozone on stretched rubber vulcanizates. I. The rate of cut growth, *J. Appl. Polym. Sci.*, 3, 90–99, 1960.
- Cullen, J. and Neale, P.: Ultraviolet radiation, ozone depletion, and marine photosynthesis, *Photosynth. Res.*, 39, 303–320, doi:10.1007/bf00014589, 1994.
- Darby, S. B., Smith, P. D., and Venables, D. S.: Cavity-enhanced absorption using an atomic line source: application to deep-UV measurements, *Analyst*, 137, 2318–2321, 2012.
- Fiedler, S. E., Hese, A., and Ruth, A. A.: Incoherent broad-band cavity-enhanced absorption spectroscopy, *Chem. Phys. Lett.*, 371, 284–294, doi:10.1016/S0009-2614(03)00263-X, 2003.

## Fast response cavity enhanced ozone monitor

A. L. Gomez and  
E. P. Rosen

Title Page

Abstract

Introduction

Conclusions

References

Tables

Figures

⏪

⏩

◀

▶

Back

Close

Full Screen / Esc

Printer-friendly Version

Interactive Discussion



## Fast response cavity enhanced ozone monitor

A. L. Gomez and  
E. P. Rosen

Title Page

Abstract

Introduction

Conclusions

References

Tables

Figures

⏪

⏩

◀

▶

Back

Close

Full Screen / Esc

Printer-friendly Version

Interactive Discussion



Finlayson-Pitts, B. J. and Pitts Jr., J. N.: Tropospheric air pollution: ozone, airborne toxics, polycyclic aromatic hydrocarbons, and particles, *Science*, 276, 1045–1051, doi:10.1126/science.276.5315.1045, 1997.

Fuhrer, J. and Booker, F.: Ecological issues related to ozone: agricultural issues, *Environ. Int.*, 29, 141–154, doi:10.1016/s0160-4120(02)00157-5, 2003.

Gauderman, W. J., Gilliland, G. F., Vora, H., Avol, E., Stram, D., McConnell, R., Thomas, D., Lurmann, F., Margolis, H. G., Rappaport, E. B., Berhane, K., and Peters, J. M.: Association between air pollution and lung function growth in Southern California children: results from a second cohort, *Am. J. Resp. Crit. Care*, 166, 76–84, doi:10.1164/rccm.2111021, 2002.

Gherman, T., Venables, D. S., Vaughan, S., Orphal, J., and Ruth, A. A.: Incoherent broadband cavity-enhanced absorption spectroscopy in the near-ultraviolet: application to HONO and NO<sub>2</sub>, *Environ. Sci. Technol.*, 42, 890–895, 2008.

Komhyr, W. D.: Electrochemical concentration cells for gas analysis, *Ann. Geophys.*, 25, 203–210, 1969, <http://www.ann-geophys.net/25/203/1969/>.

Molina, L. T. and Molina, M. J.: Absolute absorption cross sections of ozone in the 185- to 350-nm wavelength range, *J. Geophys. Res.*, 91, 14501–14508, doi:10.1029/JD091iD13p14501, 1986.

Molina, M. J. and Rowland, F. S.: Stratospheric sink for chlorofluoromethanes: chlorine atom-catalysed destruction of ozone, *Nature*, 249, 810–812, 1974.

Ridley, B. A., Grahek, F. E., and Walega, J. G.: A small high-sensitivity, medium-response ozone detector suitable for measurements from light aircraft, *J. Atmos. Ocean. Tech.*, 9, 142–148, doi:10.1175/1520-0426(1992)009<0142:ashsmr>2.0.co;2, 1992.

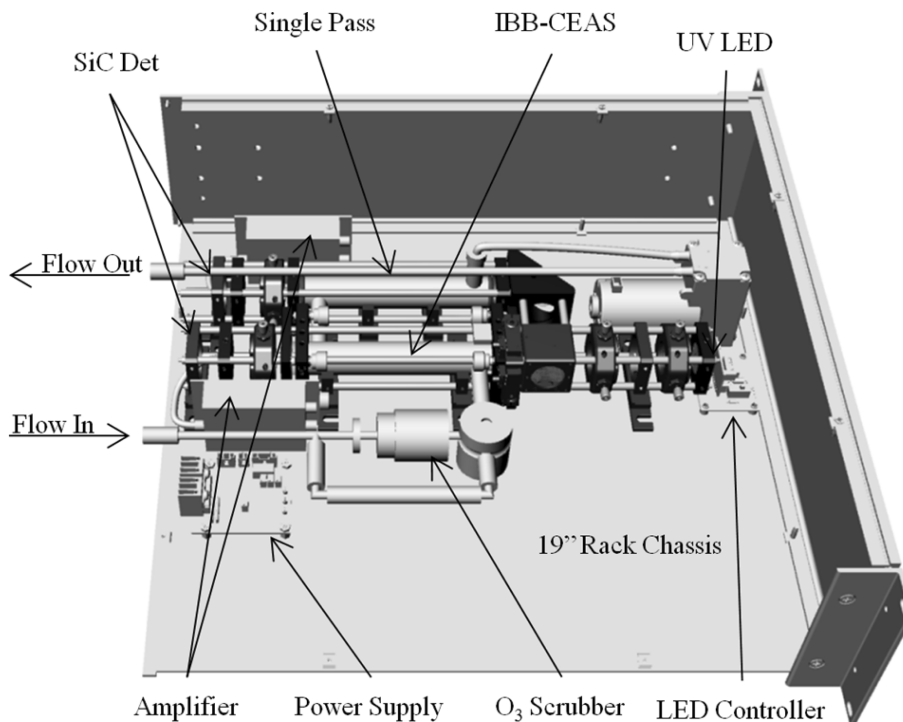
Sillman, S.: The relation between ozone, NO<sub>x</sub> and hydrocarbons in urban and polluted rural environments, *Atmos. Environ.*, 33, 1821–1845, doi:10.1016/s1352-2310(98)00345-8, 1999.

Venables, D. S., Staak, M., and Ruth, A. A.: Broadband cavity-enhanced absorption spectroscopy for trace gas detection, *Opto-Ireland 2005: Optical Sensing and Spectroscopy*, Proc. SPIE, 5826, 202–211, doi:10.1117/12.605111, 2005.

Vömel, H. and Diaz, K.: Ozone sonde cell current measurements and implications for observations of near-zero ozone concentrations in the tropical upper troposphere, *Atmos. Meas. Tech.*, 3, 495–505, doi:10.5194/amt-3-495-2010, 2010.

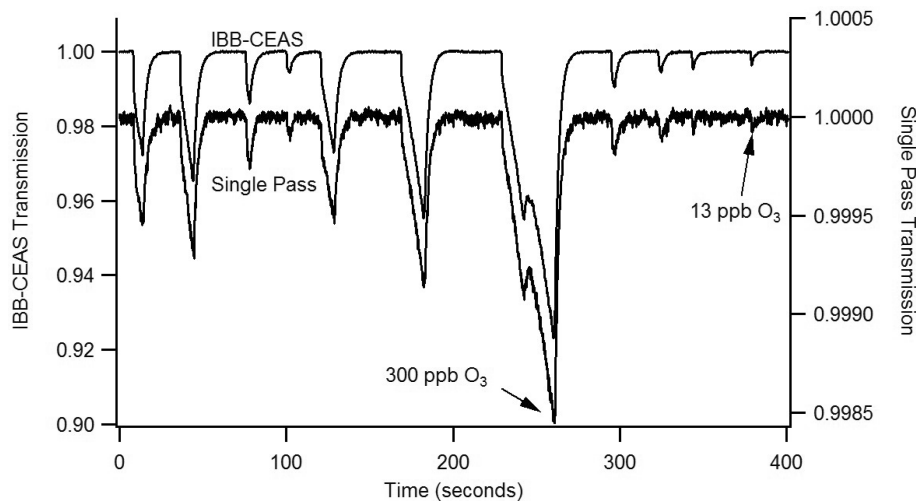
**Fast response cavity enhanced ozone monitor**A. L. Gomez and  
E. P. Rosen[Title Page](#)[Abstract](#)[Introduction](#)[Conclusions](#)[References](#)[Tables](#)[Figures](#)[⏪](#)[⏩](#)[◀](#)[▶](#)[Back](#)[Close](#)[Full Screen / Esc](#)[Printer-friendly Version](#)[Interactive Discussion](#)

- Washenfelder, R. A., Wagner, N. L., Dube, W. P., and Brown, S. S.: Measurement of atmospheric ozone by cavity ring-down spectroscopy, *Environ. Sci. Technol.*, 45, 2938–2944, doi:10.1021/es103340u, 2011.
- 5 Wennberg, P. O., Cohen, R. C., Stimpfle, R. M., Koplrow, J. P., Anderson, J. G., Salawitch, R. J., Fahey, D. W., Woodbridge, E. L., Keim, E. R., Gao, R. S., Webster, C. R., May, R. D., Toohey, D. W., Avallone, L. M., Proffitt, M. H., Loewenstein, M., Podolske, J. R., Chan, K. R., and Wofsy, S. C.: Removal of stratospheric O<sub>3</sub> by radicals: in situ measurements of OH, HO<sub>2</sub>, NO, NO<sub>2</sub>, ClO, and BrO, *Science*, 266, 398–404, doi:10.1126/science.266.5184.398, 1994.
- 10 Wu, T., Zhao, W. X., Li, J. S., Zhang, W. J., Chen, W. D., and Gao, X. M.: Incoherent broadband cavity enhanced absorption spectroscopy based on LED, *Guang Pu Xue Yu Guang Pu Fen Xi*, 28, 2469–2472, 2008.
- Zahn, A., Weppner, J., Widmann, H., Schlote-Holubek, K., Burger, B., Kühner, T., and Franke, H.: A fast and precise chemiluminescence ozone detector for eddy flux and airborne application, *Atmos. Meas. Tech.*, 5, 363–375, doi:10.5194/amt-5-363-2012, 2012.

**Fast response cavity enhanced ozone monitor**A. L. Gomez and  
E. P. Rosen

**Fig. 1.** Rendering of simultaneous IBB-CEAS and single-pass ozone measurement system in a standard 19" rack-mount chassis.

[Title Page](#)[Abstract](#)[Introduction](#)[Conclusions](#)[References](#)[Tables](#)[Figures](#)[◀](#)[▶](#)[◀](#)[▶](#)[Back](#)[Close](#)[Full Screen / Esc](#)[Printer-friendly Version](#)[Interactive Discussion](#)

**Fast response cavity enhanced ozone monitor**A. L. Gomez and  
E. P. Rosen

**Fig. 2.** Simultaneous 0.1 s integration IBB-CEAS and single pass transmission measurements of periodic ozone introductions.

[Title Page](#)[Abstract](#)[Introduction](#)[Conclusions](#)[References](#)[Tables](#)[Figures](#)[◀](#)[▶](#)[◀](#)[▶](#)[Back](#)[Close](#)[Full Screen / Esc](#)[Printer-friendly Version](#)[Interactive Discussion](#)

**Fast response cavity enhanced ozone monitor**A. L. Gomez and  
E. P. Rosen

Title Page

Abstract

Introduction

Conclusions

References

Tables

Figures

◀

▶

◀

▶

Back

Close

Full Screen / Esc

Printer-friendly Version

Interactive Discussion

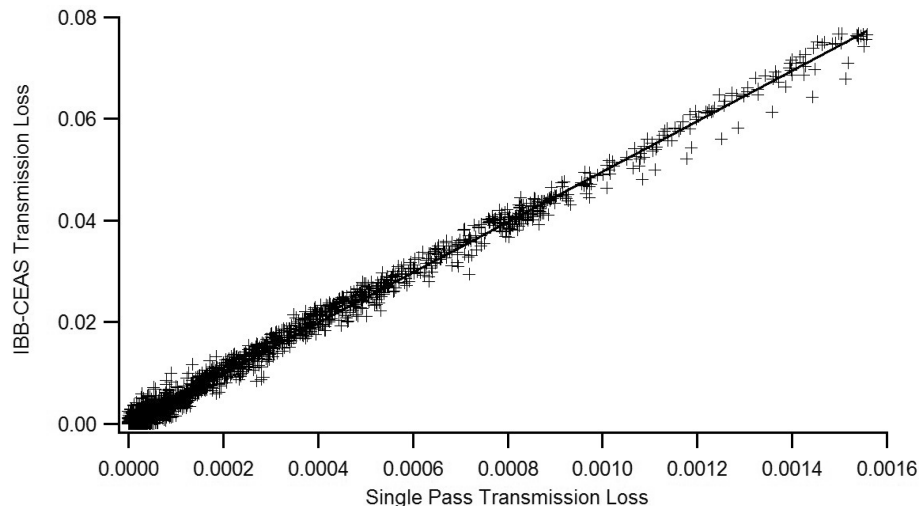


**Fig. 3.** Measured transmission losses for IBB-CEAS vs. single pass sample cells with matching ozone concentrations, indicating an enhancement value of  $50\times$ . Scatter is due to noise in the single pass measurements used in the calculation (see Fig. 2).

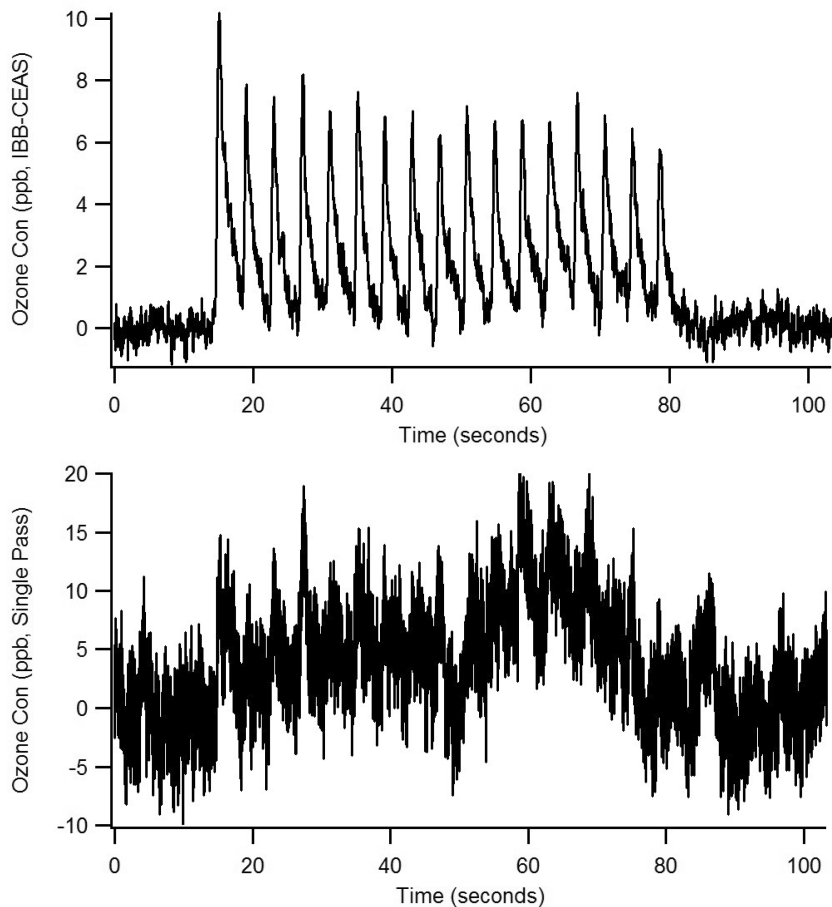


**Fig. 4.** Simultaneous IBB-CEAS (top) and single pass (bottom) transmission measurements taken at 0.001 s integration, of periodic ozone concentration spikes generated from discrete Hg lamp pulses.

**Fast response cavity enhanced ozone monitor**

A. L. Gomez and  
E. P. Rosen

[Title Page](#)

[Abstract](#)   [Introduction](#)

[Conclusions](#)   [References](#)

[Tables](#)   [Figures](#)

[◀](#)   [▶](#)

[◀](#)   [▶](#)

[Back](#)   [Close](#)

[Full Screen / Esc](#)

[Printer-friendly Version](#)

[Interactive Discussion](#)



## Fast response cavity enhanced ozone monitor

A. L. Gomez and  
E. P. Rosen

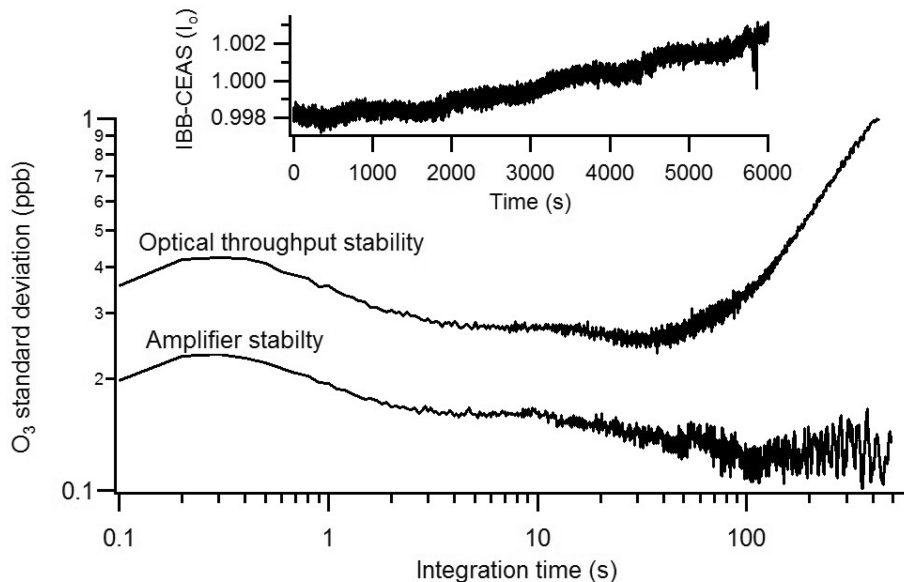


**Fig. 5.** Allan deviation analysis to determine improvement gains from data averaging, and the time domain for re-zeroing of the background to attain a targeted precision.

Title Page

Abstract

Introduction

Conclusions

References

Tables

Figures

⏪

⏩

◀

▶

Back

Close

Full Screen / Esc

Printer-friendly Version

Interactive Discussion